# SCIENTIFIC DATA (110110)

# **OPEN**

# **SUBJECT CATEGORIES**

» Outcomes research» Neurology

Received: 30 June 2015 Accepted: 04 January 2016 Published: 2 February 2016

# A structural and functional magnetic resonance imaging dataset of brain tumour patients

Cyril R. Pernet<sup>1,2</sup>, Krzysztof J. Gorgolewski<sup>3</sup>, Dominic Job<sup>1,2</sup>, David Rodriguez<sup>1,2</sup>, Ian Whittle<sup>1,2,4</sup> & Joanna Wardlaw<sup>1,2</sup>

We collected high resolution structural (T1, T2, DWI) and several functional (BOLD T2\*) MRI data in 22 patients with different types of brain tumours. Functional imaging protocols included a motor task, a verb generation task, a word repetition task and resting state. Imaging data are complemented by demographics (age, sex, handedness, and pathology), behavioural results to motor and cognitive tests and direct cortical electrical stimulation data (pictures of stimulation sites with outcomes) performed during surgery. Altogether, these data are suited to test functional imaging methods for single subject analyses, in particular methods that focus on locating eloquent cortical areas, critical functional and/or structural network hubs, and predict patient status based on imaging data (presurgical mapping).

Design Type(s)	repeated measure design • disease state design				
Measurement Type(s)	nuclear magnetic resonance assay				
Technology Type(s)	MRI Scanner				
Factor Type(s)	Diagnosis • Anatomical_location				
Sample Characteristic(s)	Homo sapiens • brain				

<sup>1</sup>Brain Research Imaging Centre, The University of Edinburgh, Edinburgh EH4 2XU, UK. <sup>2</sup>Centre for Clinical Brain Sciences, The University of Edinburgh, Edinburgh EH16 4SB, UK. <sup>3</sup>Department of Psychology, Stanford University, Stanford, California 94305, USA. <sup>4</sup>Division of Clinical Neuroscience, NHS-Lothian, Edinburgh EH4 2XU, UK. Correspondence and requests for materials should be addressed to C.R.P. (email: cyril.pernet@ed.ac.uk).

# **Background & summary**

Soon after its inception, functional Magnetic Resonance Imaging (fMRI) was used to guide brain tumour surgery<sup>1</sup>, and it is nowadays used in almost all areas of neurology research, from developmental to psychiatric disorders, dementia and stroke<sup>2</sup>. Despite this popularity in clinical research and its promising utility for surgical planning<sup>3</sup>, it is not used extensively in day to day clinical practice because, among other factors, of its limited accuracy, so far, at delineating eloquent areas in single subjects (but see Gorgolewski *et al.*<sup>4,5</sup>). The clinical data presented here were acquired in the context of a pilot study examining the feasibility and utility of fMRI for brain tumour surgical planning, with the aim of developing and validating techniques to translate fMRI cognitive paradigms to improved clinical outcomes<sup>6</sup>. Importantly, these clinical data can also be compared with another freely available dataset obtained in healthy volunteers, which used the exact same MRI protocol<sup>7</sup>.

Collecting and analysing data from brain tumour patients is challenging because of: (i) the variety of tumour types and locations; (ii) the variety of behavioural and cognitive deficits observed pre- and post-surgery, even for patients that have the same tumour type and at similar locations; and (iii) the almost unavoidable missing data, due to prioritising (for obvious ethical reasons) patients health over research data acquisition. For these reasons there are very few other MRI clinical data available, beside the Multimodal Brain Tumour Image Segmentation Benchmark data<sup>8</sup> which are useful for structural imaging method development. The data presented here are well suited to test functional imaging methods for single subjects, in particular methods that focus on locating eloquent cortical areas, critical functional and structural network hubs, and predict patient status (recovery versus additional deficits caused by surgery versus behavioural improvement) based on imaging data. They can also be used to examine integrated measurements (task based fMRI, with resting state fMRI and Diffusion Tensor Imaging (DTI) network analysis) to investigate issues of brain plasticity and associated behavioural performances at the group level, therefore serving both the biomedical and data science communities.

### Methods

The study was approved by the NHS Lothian South East Scotland Research Ethics Committee (REC reference number: 05/S1104/45). Patients gave informed consent for the study, including sharing of anonymised data, for non-commercial purposes (annex 1).

### Patient recruitment

Patients (9 Females, 13 Males, aged 25 to 75) were recruited by IW during his clinical consultations. Patients were asked to participate in the study when (i) they had a tumour located in or near a potentially eloquent area that could be mapped (motor cortex, Broca area, auditory cortex and Wernicke area) and (ii) their case posed problems in planning the surgery (e.g., deep tumour presumed to be located under/behind an eloquent area). There were no other inclusion or exclusion criteria. Most tumours were located around the pre-central region above the temporal plane (see Figure 1).

# Imaging data

Data were acquired on a GE Signa HDxt 1.5 Tesla scanner with an 8 channel phased-array head coil at the Brain Research Imaging Centre, University of Edinburgh, UK. Structural Imaging Data includes high resolution T1-weighted and T2-weighted MRI data collected along with Diffusion weighted imaging suitable for diffusion tensor imaging. Functional Imaging Data include up to 4 protocols per patient: motor task, verb generation task, word repetition task and resting state (an example of data is shown Figure 2, see Table 1 for details). Prior to using these protocols on a clinical population, we validated them in ten healthy controls using a test-retest design<sup>4</sup> to identify tests that were reliable at the single subject level. As mentioned above, data from this study are also publicly available<sup>7</sup> and can be combined with the currently presented dataset. Functional MRI stimuli were presented using the Nordic Neurolab visual and auditory system. Presentation software was used to code the different protocols. The code and stimuli are also available, along with the aforementioned test-retest dataset. Image acquisition parameters for structural and functional data are outlined in Table 2.

T1 and T2 images were defaced using SPM12, i.e., after computing the affine transform to standard space, the whole area from the forehead to the throat was removed (nullified). Tissue classes and volume estimates are also made available. For each subject, a mask of the tumour and oedema was generated semi-automatically using MRIcron 3D fill tool on the T1 and/or T2 images. This mask was then warped into standard space by estimating deformation form the T1 which allowed to create a new *a priori* tissue class. Data were then segmented using the 'new segment' in SPM12 using the standard priors from the MNI template, augmented by the new tumour class. Volume estimates were computed based on the segmented data and wrapping field obtained as part of the SPM segmentation.

## Direct electrical stimulation

DES during neurosurgery was performed in 17 patients. Patients were first anesthetized using propofol or fentanyl in infusion, followed by craniotomy to expose the cortex over and around the tumour using image guidance, and then wakened for DES while in the operating theatre Figure 2. When the electrical current is applied over primary sensory-motor areas, a positive outcome is expected. In the current study, DES over the different parts of the primary motor cortex was expected to induce movements in the

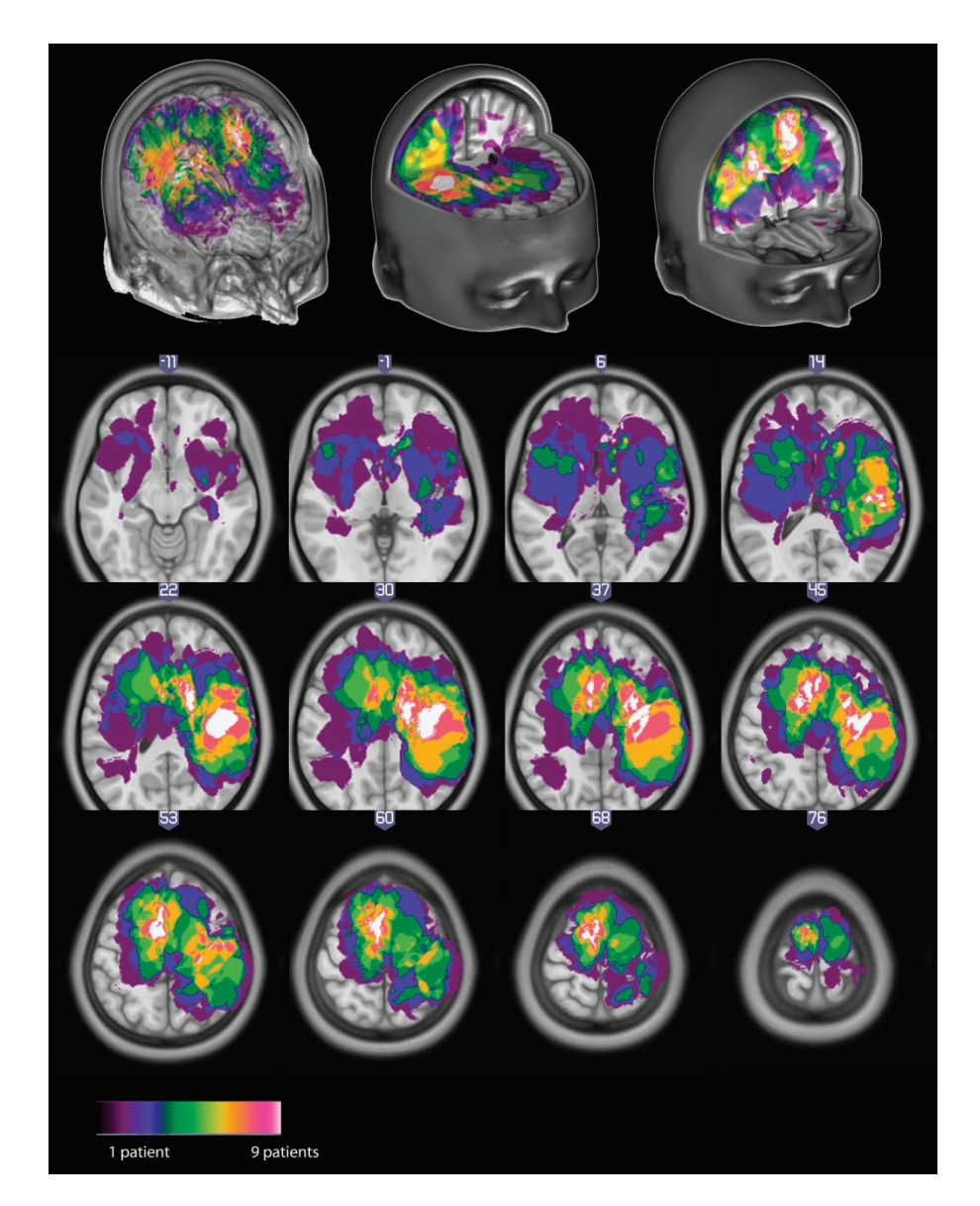
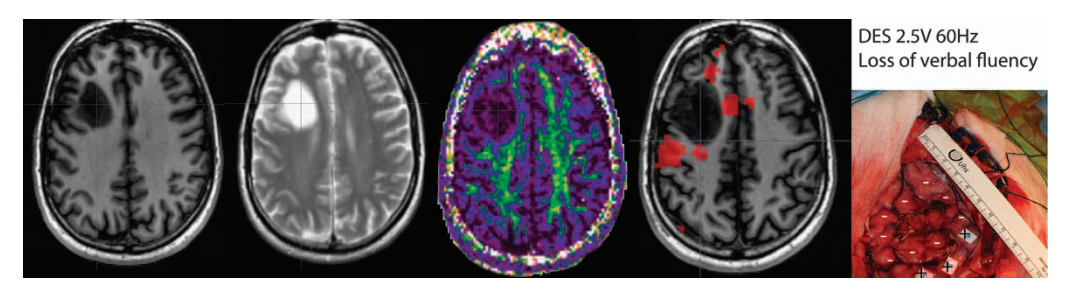


Figure 1. Distribution of tumours across all patients, displayed in MNI space using neurological convention.



**Figure 2.** From left to right, the first 3 images show structural data: T1-weighted, T2-weighted, Diffusion weighted (Fractional Anisotropy map here) images. These data are complemented by functional BOLD imaging and Direct Electrical Stimulation.

associated boby parts. When DES is applied over secondary and associative areas, a negative outcome is expected. In the current study, stimulation of Wernicke or Broca area, a speech impairment or arrest was expected. For each patient undergoing DES procedure a digital photograph of the exposed cortex was taken (prior to the tumour resection), annotated with stimulation sites and the effect of the electrical

		0,	Tumour Location	Volume	Structural	Functional	DES
18638	R	Astrocytoma type II	Right primary somatosensory area	ght primary somatosensory area 0.056 T1-T2-DTI		М	Y
19227	R	Astrocytoma type II	a type II Right primary somatosensory area 0.068 DTI		DTI	M-V-W	Y
18886	L	Astrocytoma type II Right Insula 0.189 T1-T2-DTI		M-V-R	Y		
19567	R	Astrocytoma type II	trocytoma type II Left Pre-Motor area 0.038 T1-T2-DTI		M-V-W	Y	
18582	R	Astrocytoma type II	Astrocytoma type II Wernicke area 0.021 T1-		T1-T2-DTI	M-V-W	N
19723	L	Astrocytoma type II	strocytoma type II Left temporal cortex		T1-T2-DTI	MV-W-R	Y
18428	R	Astrocytoma type III	Astrocytoma type III Right Supplementary Motor Area 0.054		T1-T2-DTI	M-R	Y
19423	R	Glioblastoma Multiform Right primary motor area		0.112	T1-T2-DTI	M-R	Y
19357	R	Glioblastoma Multiform Right primary motor area		0.099	T1-T2-DTI	M-R	N
18975	R	Glioblastoma Multiform	oblastoma Multiform Left primary motor area		T1-T2-DTI	M-V-W-R	Y
19015	R	Glioblastoma Multiform	lastoma Multiform		T1-T2-DTI	M-V-W	Y
18756	R	Glioblastoma Multiform	m Right primary motor area 0.056 T1-T2-D7		T1-T2-DTI	M-R	Y
18716	R	Glioblastoma Multiform	m Right primary motor area 0.096		T1-T2-DTI	M-V-W	N
19085	R	Meningioma	Right Supplementary Motor Area		T1-T2-DTI	M-R	Y
19275	R	Meningioma	na Right Pre-Motor Area		T1-T2-DTI	М	N
19628	R	Meningioma	ioma Left Pre-Motor area		T1-T2-DTI	M-V-W-R	N
18675	R	Meningioma	Left primary motor area 0.104		T1-T2-DTI	M-V-W	Y
19691	R	Oligodendrocytoma type II	Right Pre-Motor area 0.037 T1-T2-DTI		M-R	Y	
17904	R	Oligodendrocytoma type II	Left Supplementary Motor Area 0.031 T1-T2-DTI		M-V-R	Y	
19849	R	nil	Right primary motor area 0.007 T1-T2		M-R	Y	
19398	R	Met lung CA	Right primary somatosensory area 0.064 T1-T2-DTI		T1-T2-DTI	M-R	Y
18863	L	renal cell carcinoma	Left Pre-Motor Area 0.104 T1-T2-DTI M-V		M-V-W	Y	
	18886 19567 188882 19723 18428 19423 199357 188756 18756 18756 19085 19275 199628 18675 199628 18675 199691 17904	18886 L 19567 R 18582 R 19723 L 18428 R 19423 R 19423 R 199357 R 18975 R 18975 R 19015 R 18756 R 18756 R 18756 R 19275 R 19628 R 18675 R 19691 R 17904 R 19849 R	18886 L Astrocytoma type II 19567 R Astrocytoma type II 18582 R Astrocytoma type II 19723 L Astrocytoma type II 18428 R Astrocytoma type III 19423 R Glioblastoma Multiform 19357 R Glioblastoma Multiform 18975 R Glioblastoma Multiform 18975 R Glioblastoma Multiform 1876 R Glioblastoma Multiform 1876 R Glioblastoma Multiform 18776 R Glioblastoma Multiform 19085 R Meningioma 19275 R Meningioma 19275 R Meningioma 19488 R Meningioma 19488 R Meningioma 19588 R Meningioma 19588 R Meningioma 19691 R Oligodendrocytoma type II 17904 R Oligodendrocytoma type II 17904 R Oligodendrocytoma type II 199849 R nil	18886 L Astrocytoma type II Right Insula 19567 R Astrocytoma type II Left Pre-Motor area 18582 R Astrocytoma type II Wernicke area 19723 L Astrocytoma type II Left temporal cortex 18428 R Astrocytoma type III Right Supplementary Motor Area 19423 R Glioblastoma Multiform Right primary motor area 19357 R Glioblastoma Multiform Right primary motor area 18975 R Glioblastoma Multiform Left Supplementary Motor Area 18976 R Glioblastoma Multiform Right primary motor area 1876 R Glioblastoma Multiform Right primary motor area 1876 R Glioblastoma Multiform Right primary motor area 1876 R Glioblastoma Multiform Right primary motor area 1877 R Meningioma Right Pre-motor area 19085 R Meningioma Right Pre-Motor Area 19275 R Meningioma Left Pre-Motor Area 19275 R Meningioma Left Pre-Motor area 19628 R Meningioma Left Pre-Motor area 19691 R Oligodendrocytoma type II Right Pre-Motor area 19691 R Oligodendrocytoma type II Left Supplementary Motor Area 19704 R Oligodendrocytoma type II Left Supplementary Motor Area 19849 R nil Right primary motor area	18886 L Astrocytoma type II Right Insula 0.189 19567 R Astrocytoma type II Left Pre-Motor area 0.038 18582 R Astrocytoma type II Wernicke area 0.021 19723 L Astrocytoma type III Left temporal cortex 0.091 18428 R Astrocytoma type III Right Supplementary Motor Area 0.054 19423 R Glioblastoma Multiform Right primary motor area 0.112 19357 R Glioblastoma Multiform Right primary motor area 0.099 18975 R Glioblastoma Multiform Left primary motor area 0.017 19015 R Glioblastoma Multiform Left Supplementary Motor Area 0.03 18756 R Glioblastoma Multiform Right primary motor area 0.056 18716 R Glioblastoma Multiform Right primary motor area 0.096 19085 R Meningioma Right Supplementary Motor Area 0.052 19275 R Meningioma Right Pre-Motor Area 0.051 19288 R Meningioma Left Pre-Motor Area 0.031 19628 R Meningioma Left Pre-Motor area 0.164 19691 R Oligodendrocytoma type II Right Pre-Motor area 0.037 17904 R Oligodendrocytoma type II Right primary motor area 0.037 17904 R Oligodendrocytoma type II Left Supplementary Motor Area 0.031 19398 R Met lung CA Right primary somatosensory area 0.064	8886 L Astrocytoma type II Right Insula 0.189 T1-T2-DT1  8582 R Astrocytoma type II Left Pre-Motor area 0.038 T1-T2-DT1  8582 R Astrocytoma type II Wernicke area 0.021 T1-T2-DT1  8428 R Astrocytoma type III Right Supplementary Motor Area 0.054 T1-T2-DT1  8428 R Astrocytoma type III Right Supplementary Motor Area 0.054 T1-T2-DT1  9923 R Glioblastoma Multiform Right primary motor area 0.112 T1-T2-DT1  99357 R Glioblastoma Multiform Right primary motor area 0.099 T1-T2-DT1  8975 R Glioblastoma Multiform Left primary motor area 0.017 T1-T2-DT1  8976 R Glioblastoma Multiform Left Supplementary Motor Area 0.03 T1-T2-DT1  8776 R Glioblastoma Multiform Right primary motor area 0.036 T1-T2-DT1  8776 R Glioblastoma Multiform Right primary motor area 0.056 T1-T2-DT1  8776 R Glioblastoma Multiform Right primary motor area 0.056 T1-T2-DT1  8776 R Glioblastoma Multiform Right primary motor area 0.056 T1-T2-DT1  8776 R Glioblastoma Multiform Right primary motor area 0.056 T1-T2-DT1  8776 R Glioblastoma Multiform Right primary motor area 0.070 T1-T2-DT1  8776 R Meningioma Right Pre-Motor Area 0.031 T1-T2-DT1  8777 R Meningioma Left Pre-Motor area 0.040 T1-T2-DT1  9787 R Meningioma Left Pre-Motor area 0.041 T1-T2-DT1  9788 R Meningioma Left Pre-Motor area 0.047 T1-T2-DT1  9789 R Oligodendrocytoma type II Right Pre-Motor area 0.031 T1-T2-DT1  9789 R Oligodendrocytoma type II Right Pre-Motor area 0.007 T1-T2-DT1  9789 R Met lung CA Right primary motor area 0.064 T1-T2-DT1	8886 L Astrocytoma type II Right Insula 0.189 T1-T2-DTI M-V-W 99567 R Astrocytoma type II Left Pre-Motor area 0.038 T1-T2-DTI M-V-W 8582 R Astrocytoma type II Wernicke area 0.021 T1-T2-DTI M-V-W 99723 L Astrocytoma type II Left temporal cortex 0.091 T1-T2-DTI M-V-W-R 8428 R Astrocytoma type III Right Supplementary Motor Area 0.054 T1-T2-DTI M-R 99423 R Glioblastoma Multiform Right primary motor area 0.112 T1-T2-DTI M-R 99425 R Glioblastoma Multiform Right primary motor area 0.099 T1-T2-DTI M-R 18975 R Glioblastoma Multiform Left primary motor area 0.099 T1-T2-DTI M-V-W-R 18975 R Glioblastoma Multiform Left Supplementary Motor Area 0.03 T1-T2-DTI M-V-W-R 18766 R Glioblastoma Multiform Right primary motor area 0.037 T1-T2-DTI M-V-W-R 18756 R Glioblastoma Multiform Right primary motor area 0.056 T1-T2-DTI M-V-W-R 18756 R Glioblastoma Multiform Right primary motor area 0.056 T1-T2-DTI M-V-W-R 18756 R Glioblastoma Multiform Right primary motor area 0.056 T1-T2-DTI M-V-W-W-R 18756 R Glioblastoma Multiform Right Primary motor area 0.056 T1-T2-DTI M-V-W-W-R 18756 R Meningioma Right Supplementary Motor Area 0.052 T1-T2-DTI M-V-W-W-R 19085 R Meningioma Right Pre-Motor Area 0.031 T1-T2-DTI M-V-W-R 19085 R Meningioma Left Primary motor area 0.031 T1-T2-DTI M-V-W-R 1908675 R Meningioma Left Primary motor area 0.037 T1-T2-DTI M-V-W-R 190969 R Oligodendrocytoma type II Right Pre-Motor Area 0.031 T1-T2-DTI M-V-W-R 19099 R Oligodendrocytoma type II Left Supplementary Motor Area 0.031 T1-T2-DTI M-V-W-R 19099 R Met lung CA Right primary somatosensory area 0.064 T1-T2-DTI M-V-W-R

**Table 1.** Patients' information with handedness, pathology obtained from histology (nil if not obtained), tumour location and volume, and details of the MRI sequences obtained along with DES. Sex and age are also available with the data but not presented here to avoid possible identification.

stimulation. The presence/absence of significant fMRI activations compared to the effect of DES allowed to demonstrate here a good correspondence between techniques<sup>6</sup> when using an adaptive thresholding method<sup>4</sup>.

# Behavioural data

Data were collected pre- and post-surgery by IW to evaluate impairments before surgery, and evaluate changes following surgery. The assessment of arm and hand function for both the dominant and non-dominant hands was performed using the nine hole peg test (9HPT), while assessment of lower limbs function was performed using a timed 10 meters walk. Five cognitive tests were also performed. The National Adult Reading Test (NART) was used to estimate premorbid intelligence levels of English-speaking patients. The Rey Adult Verbal learning test (RAVLT) was used to evaluating verbal learning and memory. The Williams delayed recall test (WDRT) was used to also provide an estimate of memory performance. The trail making test (TMT) was used to provide information about visual search speed, scanning, mental flexibility and executive functioning. Finally, the controlled oral word association test (COWAT) was used to test verbal fluency. Table 3 (available online only) details which tests were performed in which subjects pre- and post- surgery.

Sequence	T1	T2	DWI	Motor task	Word repetition	Verb generation	Resting state		
Pulse type	3D IRP (inversion recovery prepared)	FAST spin- echo	single-shot spin-echo EPI	single-shot gradient-echo EPI					
In plane FOV	256×256 mm								
In plane matrix	256 × 256		128×128	64×64					
Slice thickness	1.3 mm		2 mm	4 mm					
Number of slices	156		72	30					
Acquisition order	front to back	to	pp to bottom	interleaved					
Slice orientation	coronal		axial	axial (AC-PC)					
TR	10 s	2.5 s	16.5 s	5 s	2.5 s				
TE	4 s	102 ms	98 ms	50 ms					
Excitation flip angle	8	90	90	90					
Sparse sampling	n/a	n/a	n/a	2.5 s	n/a	n/a	n/a		
Nb of volumes in the time series	1	1	71 $(7 \times b = 0 \text{ and } 64 \times b = 1,000 \text{ s/mm2})$	76	173	184	120		

Table 2. Summary of MRI sequences and parameters.

#### **Data Records**

The data are available through the UK data service (http://ukdataservice.ac.uk/) under collection name: 'A neuroimaging dataset of brain tumour patients' (Data Citation 1).

# Demographics and behavioural data

These are considered as metadata, informing the imaging data. There is one metadata.pdf summarizing the data and a metadata.xlsx file (and the corresponding MRI\_DES\_data.csv and clinical\_data.csv files). In this excel or csv files the age, sex, actual score values to tests and dates of these exam are provided.

# Imaging data

Data from each patient is available as a tar file with the ID provided in Table 1. Inside the archive is a folder with sub-ID which contains the data organized as zip files. Each zip file names reflects the order in which data were acquired and the sequence name. For instance, 5\_finger\_foot\_lips.zip, 7\_resting\_state.zip, 8\_Axial\_T2.zip, 10\_cor\_3D\_IR\_PREP.zip, 10\_DTI\_64G\_2.0-mm\_isotropic.zip indicates that we started by the fMRI motor task, then resting state and moved onto structural imaging. Note that when DTI was obtained, the average diffusion coefficient, fractional anisotropy, and traceotropic maps were computed automatically by the scanner and made also available here. Finally, there is tissue\_classes.zip file which contains the gray, white, csf and tumour tissue images in subject space along with a y\*.nii file which corresponds t the deformation field that can be applied to transform data into MNI space). All structural and functional data are in NIfTI format (http://nifti.nimh.nih.gov/). All imaging data have been de-identified, and structural MRI data (T1, T2) were defaced.

### Direct electrical stimulation

Along with the imaging data, there is a DES.zip file that contains pictures (.jpg) taken during surgery, indicating sites of stimulation, along with a pdf file specifying additional information like e.g., left/right/front/back.

# **Technical Validation**

Diffusion weighted data and functional MRI protocols used in this study were validated in a set of 10 healthy participants, showing reliable patterns in a test-retest setting. For DTI, we showed that reliable single subject network metric can be obtained from the sequences used<sup>9</sup>. For fMRI data, we showed that tasks used have a high single subject reliability<sup>5</sup> providing that an adaptive thresholding method is used to account for activation shifts in globals<sup>4</sup>.

### **Usage Notes**

The imaging data are available only after registration on the UK data service and a request is made. Although the data are de-identified and faces were removed from T1 and T2 imaging data, the detailed clinical records (age, sex, tumour, behavioural deficits, etc.,) might be enough to identify individuals directly or by using database cross-linkage 11. Data are also available only for non-commercial use, as consented by patients. For these reasons, imaging data are protected by the UK national database user agreement.

# References

- Gallen, C. C., Bucholz, R. & Sobel, D. F. Intracranial neurosurgery guided by functional imaging. Surg. Neurol. 42, 523–530 (1994)
- 2. Detre, J. A. & Floyd, T. F. Functional MRI and Its Applications to the Clinical Neurosciences. The Neuroscientist 7, 64-79 (2001).
- 3. Pillai, J. J. The Evolution of Clinical Functional Imaging during the Past 2 Decades and Its Current Impact on Neurosurgical Planning. *Am. J. Neuroradiol.* **31**, 219–225 (2010).
- 4. Gorgolewski, K. J., Storkey, A. J., Bastin, M. E. & Pernet, C. R. Adaptive thresholding for reliable topological inference in single subject fMRI analysis. Front. Hum. Neurosci. 6, 245 (2012).
- Gorgolewski, K. J., Storkey, A. J., Bastin, M. E., Whittle, I. & Pernet, C. Single subject fMRI test–retest reliability metrics and confounding factors. NeuroImage 69, 231–243 (2013).
- Pernet, C. R. et al. Evaluation of a pre-surgical functional MRI workflow: from data acquisition to reporting. Int. J. Med. Iinformatics 6, 37–42 (2015).
- 7. Gorgolewski, K. et al. A test-retest fMRI dataset for motor, language and spatial attention functions. GigaScience 2, 6 (2013).
- Menze, B. H. et al. The Multimodal Brain Tumour Image Segmentation Benchmark (BRATS). IEEE Trans. Med. Imaging 34, 1993–2024 (2015).
- 9. Buchanan, C. R., Pernet, C. R., Gorgolewski, K. J., Storkey, A. J. & Bastin, M. Test-retest reliability of structural brain networks from diffusion MRI. NeuroImage 86, 231–243 (2014).
- 10. Gibb, A. P. & McCallum, A. K. New Delhi metallo-β-lactamase 1. Lancet Infect. Dis. 10, 751-752 (2010).
- 11. Gymrek, M., McGuire, A. L., Golan, D., Halperin, E. & Erlich, Y. Identifying Personal Genomes by Surname Inference. *Science* 339, 321–324 (2013).

#### **Data Citation**

1. Pernet, C., Gorgolewski, K. & Whittle, I. UK Data Archive. http://dx.doi.org/10.5255/UKDA-SN-851861 (2016).

# **Acknowledgements**

The data acquisition was funded by Cancer Research UK through the Edinburgh Experimental Cancer Medical Centre.

# **Author Contributions**

C.R.P.: conception and design of the study, data organization, de-identification and curation, drafting of the article. K.J.G.: data acquisition, critical review and final approval of the version submitted. D.J.: data curation, critical review and final approval of the version submitted. D.R.: data de-identification, critical review and final approval of the version submitted. I.W.: conception and design of the study, acquisition of data, and final approval of the version submitted. J.W.: conception of the study, clinical translation standards, critical review and final approval of the version submitted.

# **Additional Information**

Table 3 is only available in the online version of this paper.

**Competing financial interests:** The authors declare no competing financial interests.

How to cite this article: Pernet, C. R. et al. A structural and functional magnetic resonance imaging dataset of brain tumour patients. Sci. Data 3:160003 doi: 10.1038/sdata.2016.3 (2016).

This work is licensed under a Creative Commons Attribution 4.0 International License. The images or other third party material in this article are included in the article's Creative Commons license, unless indicated otherwise in the credit line; if the material is not included under the Creative Commons license, users will need to obtain permission from the license holder to reproduce the material. To view a copy of this license, visit http://creativecommons.org/licenses/by/4.0

Metadata associated with this Data Descriptor is available at http://www.nature.com/sdata/ and is released under the CC0 waiver to maximize reuse.